



PERFORMANCE CRITERIA FOR RC HIGH-RISE WALL BUILDINGS EXPOSED TO VARIED SEISMIC SCENARIOS

W. ALWAEI⁽¹⁾, A. MWAFY⁽²⁾, K. PILAKOUTAS⁽³⁾, M. GUADAGNINI⁽⁴⁾

¹ Corresponding Author, The University of Sheffield, UK, wael.mahdi@sheffield.ac.uk

² Associate Professor, United Arab Emirates University, UAE, amanmwafy@uaeu.ac.ae

³ Professor, The University of Sheffield, UK, k.pilakoutas@sheffield.ac.uk

⁴ Senior Lecturer, The University of Sheffield, UK, m.guadagnini@sheffield.ac.uk

Abstract

As a result of population growth and consequent urbanisation, the number of high-rise buildings is rapidly growing worldwide resulting in increased exposure to multiple-scenario earthquakes and associated risks. The wide range in frequency contents of possible strong ground motions can have impact on the seismic response, vulnerability and limit state criteria definitions of RC high-rise wall structures. Motivated by the pressing need to derive more accurate fragility relations for use in seismic risk assessment and mitigation of such structures, a methodology is proposed to obtain reliable, Seismic Scenario-Structure-Based (SSSB) definitions of limit state criteria. A 30-storey wall building, located in a multi-seismic scenario study region, is utilized to illustrate the methodology. The building is designed following modern seismic code provisions and then modelled using nonlinear fibre-based approach. Uncertainty in ground motions is accounted for by the selection of forty real earthquake records representing two seismic scenarios. Seismic scenario-based building local response at increasing earthquake intensities is mapped using Multi-Record Incremental Dynamic Analyses (MRIDAs) with an improved scalar Intensity Measure (IM). Net Inter-Storey Drift (NISD) is selected as a global Damage Measure (DM) based on a parametric study involving seven buildings ranging from 20-50 stories. This DM is used to link local damage events, including shear, in the sample building to global response under different seismic scenarios. The study concludes by proposing SSSB limit state criteria and fragility relations for the sample building. The proposed methodology, limit state criteria and fragility relations is suitable for comparable RC high-rise wall buildings exposed to multiple-scenario earthquakes.

Keywords: high-rise buildings, shear walls, performance criteria, incremental dynamic analysis

1. Introduction

With changing socioeconomic conditions, rapid population growth and urbanisation, many cities all over the world have expanded rapidly in recent years. This expansion has led to a massive increase in high-rise buildings and to the spread of cities to multiple-scenario earthquake-prone regions. This increases the exposure to seismic risk, which to be accurately quantified and appropriately mitigated necessitates a better understanding of the hazard and vulnerability of this building class. The majority of high-rise buildings in most countries employ RC piers and core walls as the primary lateral-force-resisting system due to their effectiveness in providing the strength, stiffness and deformation capacity needed to meet the seismic demand. Quantitative definitions of limit state criteria form the spine to seismic vulnerability assessment needed for seismic risk analysis and mitigation for RC high-rise wall buildings. These definitions require mathematical representations of local Damage Indices (DIs), such as deformations, forces or energy, based on designated structural response levels. Therefore, suitable Damage Measures (DMs) need to be adopted to sufficiently correlate local damages (events) in the building to its global response.

The aim of this paper is to propose a methodology to obtain reliable Seismic Scenario-Structure-Based (SSSB) definitions of performance limit state criteria for RC high-rise wall buildings. The proposed methodology is illustrated on a 30-storey sample building with RC bearing-wall system located in Dubai (UAE);

a multi-scenario seismic-prone region that is taken as case study in the current work. The study concludes with proposals for new SSSB performance limit state criteria for RC high-rise wall buildings in similar seismic regions. Fig. 1 summarizes the methodology proposed in the current work.

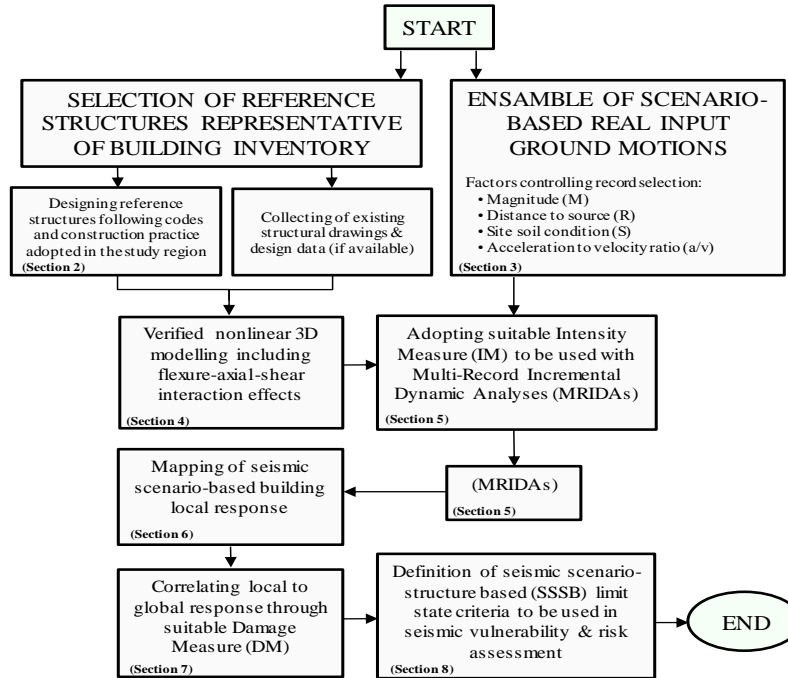


Fig. 1 – Flowchart of the proposed methodology to define SSSB limit state criteria for RC high-rise wall buildings

2. Selection and Design of Sample Building

A 30-storey, 97.3m in height, RC structure is selected as a representative sample building to define SSSB performance limit states. The footprint, layout and structural system of the building are typical in the study region for this range of height. The building consists of a bearing wall lateral force-resisting system with two basements, a ground storey, and twenty-seven typical stories. The structure is fully designed and proportioned for the purpose of this study taking into consideration modern code provisions, as well as, local authority supplementary regulations and construction practices. Based on a number of previous hazard assessment studies for the region [e.g. 1, 2], the seismic design loads are calculated using mapped spectral response accelerations of 0.85g and 0.26g at 0.2s and 1.0s, respectively, and soil class S_c (very dense soil and soft rock). These mapped acceleration parameters are adopted in the recently developed seismic maps for UAE [3]. The load combinations and design provisions of the ACI building code [4] are followed in proportioning and detailing structural members. ASTM 706 reinforcing steel is used with a yielding strength of 460MPa. The concrete strengths used in floor slabs, piers, cores and coupling beams range between 40MPa and 50MPa. Cross-sections and corresponding reinforcement of piers and cores vary along the building height. Cast-in-situ flat slabs of 0.26m thickness with periphery beams are adopted for the flooring system, also serving as a rigid diaphragm to transfer lateral forces to the vertical structural elements at each floor. The flooring system is subjected to special design requirements, including punching shear, so as to resist the combination of seismic deformations and gravity loads. Fig. 2 shows a typical floor layout of the sample building with storey labelling.

3. Seismic Scenarios and Input Ground Motions

By disaggregating the rate of occurrence associated with the level of ground motion in the Uniform Hazard Spectrum (UHS) obtained from previous studies [2, 5], Dubai is found vulnerable to two main earthquake scenarios: (i) severe distant earthquakes of magnitude 7-8 with 100-200km epicentral distance; and (ii) moderate

near-field earthquakes of magnitude 5-6 with site-to-source distance of 10-60km. To account for the uncertainty in ground excitation, the two aforementioned scenarios are represented in the present study with two sets of 20 natural earthquake records each. The European Strong-motion [6] and the Pacific Earthquake Engineering Research Centre [7] databases are used to select the earthquake records due to the insufficient number of recorded events within the study region. Fig. 3 shows the response spectra (with their means) for the two record sets alongside the response hazard spectra for 10% Probability of Exceedance in 50 years (UHS-10% POE in 50Y) and the design spectra of the study region for soil types C and D.

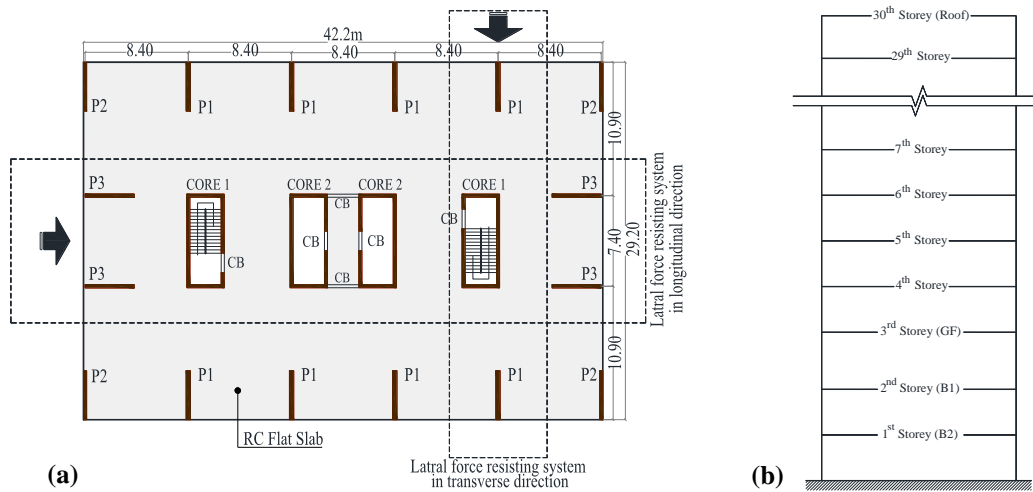


Fig. 2. – 30-storey sample building: (a) typical floor layout; and (b) storey labelling

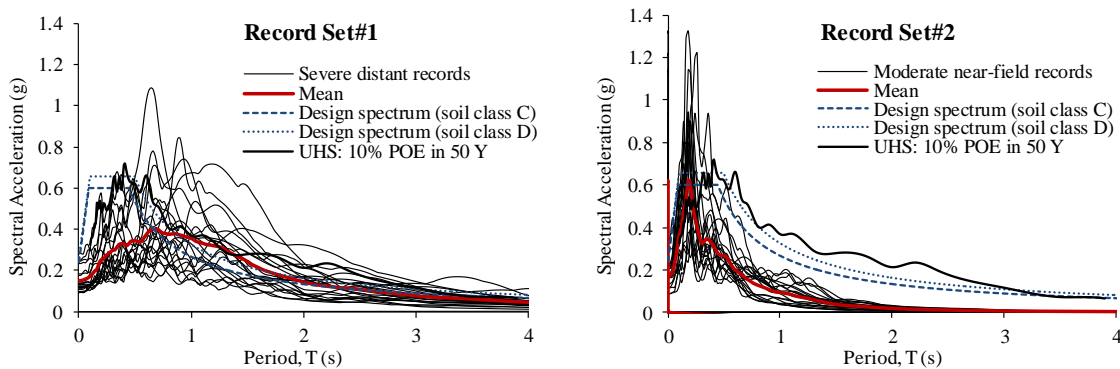


Fig. 3 – Response spectra of the 40 natural records representing severe distant (Record Set#1) and moderate near-field (Record Set#2) along with mean spectra, design spectra and 10% POE/50Y-UHS for the study region

4. Nonlinear Modelling

PERFORM-3D [8] is utilized to create the nonlinear model of the sample building. In this study, the selection of the analysis tool, modelling approach and key modelling parameters are based on a multi-level modelling verification scheme [9]. The verification scheme included the simulation of the nonlinear dynamic response of a full-scale seven-storey wall building slice tested on the LHPOST at UCSD [10, 11].

Although PERFORM-3D is an efficient 3D modelling package, it is computationally demanding to execute a large number of Nonlinear Response History Analyses (NRHAs) for a 3D model of an entire high-rise structure, particularly when a wide range of input ground motions is employed. A 3D-slice idealization is therefore adopted to develop the nonlinear model of the sample building. The results from the free vibration analysis conducted on the entire building indicate a very comparable lateral capacity in the two orthogonal directions with the fundamental mode period of 3.44s and 3.2s in the longitudinal and transverse directions,

respectively. Vindicated by this fact, the 3D slice representing the lateral-force-resisting system in the transverse direction of the sample building (Fig. 2) is modelled and employed in the subsequent sections to define SSSB Performance Limit States (PLSs). Four-noded fibre-based shear wall elements are utilized to model the piers and core wall segments while 2-noded fibre-based frame elements are used for the floor slabs. The coupling beams between the core walls are modelled as elastic beam elements with nonlinear displacement shear hinge at mid-span. The seismic masses are assigned to the nodes at storey level. The base of the sample building is rigidly modelled at the top-of-foundation level. Expected strengths of $1.3f_c'$ and $1.17f_y$, are used for concrete and reinforcing steel, respectively [12]. A four-linear-segment relation is used to approximate the concrete stress-strain relationship based on the modified Mander model [13]. For the steel in tension, the post-yield stiffness and cyclic degradation parameters are defined following adjustments described by Orakcal and Wallace [14]. For compression, buckling of steel rebar is modelled based on experimental results and analytical models from previous studies [15-18]. Inelastic shear deformation in piers and cores is accounted for by assigning a trilinear relation similar to the one given in ASCE/41-06 [19]. Test results by Thomsen and Wallace [20] and calibration studies by Gogus [21] are used to define the shear force-deformation relation. Moreover, Table 6.18 in ASCE/SEI 41-6 [2] is implemented to calculate the rotation limits of RC wall segments and coupling beams to different levels of building performance taking into consideration the level of axial and shear demands in these elements. Finally, the shear capacity of wall segments is estimated as the minimum of $1.5V_n$ [22] and $0.83 \sqrt{f_c'}$ [4]. Viscous damping in the first translational mode (fundamental mode) is accounted for by using an initial stiffness-based modal damping with 0.5% damping ratio. For computing higher mode damping, the following relationship is adopted: $\xi_i = 1.4 \xi_{(i-1)}$, where ξ_i is the damping ratio of the i^{th} mode [23]. Accordingly, the damping ratios for the next five translational modes are set to 0.7%, 1.0%, 1.4%, 1.9% and 2.7%, respectively.

5. Multi-record Incremental Dynamic Analyses

For the purpose of defining SSSB performance limit state criteria to the sample building, Multi-Record Incremental Dynamic Analyses (MRIDAs) are performed using the two sets of records described in Section 3. In the present study, an improved scalar intensity measure (IM), termed spectral acceleration at weighted-average period $S_{a(wa)}$, is proposed. The weighted-average period (T_{wa}) is the period linked to the spectral acceleration value that represents the average of the spectral acceleration ordinates corresponding to the cracked period of the first three modes of vibration weighted by their mass participation factors. The proposed IM is believed to have higher efficiency compared to S_a at first mode period as it takes into account both the impact of higher modes and period elongation. Although the sample building is assessed with MRIDAs using the 40 selected records, as shown in Fig. 4, and due to the large number of monitored DIs, a representative earthquake record is selected from each set of records to link local-to-global response in the sample building. The selected input ground motions are: (i) The 7.13M Hector Mine Earthquake of 16th October 1999 recorded at the CGS 12026 Indio-Coachella Canal station in California USA (R#5 in Record Set#1); and (ii) The 5.77M Coalinga-05 earthquake of 22nd July 1983 recorded at USGS 1606 Burnett Construction station in California USA (R#3 in Record Set#2). As can be seen in Fig. 4, the reason for choosing these records is that their IDA curves match reasonably well the 50% fractile of the IDA curves obtained from each of the two sets of records.

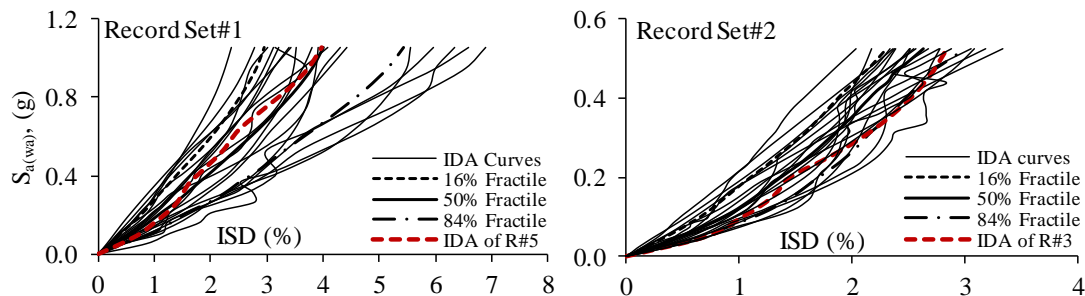


Fig. 4 – IDA curves for Record Set#1 and Record Set#2 along with their 16%, 50%, 84% fractile curves and IDA for selected record R#5 and R#3



6. Mapping of Seismic Scenario-Based Building Local Response

To determine the SSSB quantitative performance limit state definitions for the sample building, a total of seven local DIs are mapped during MRIDAs: (i) rebar yielding in slabs; (ii) rebar yielding in walls; (iii) exceeding of wall rotation limits according to ASCE/SEI 41-6; (iv) exceeding of coupling beam rotation limits according to ASCE/SEI 41-6; (v) rebar buckling in walls; (vi) concrete crushing in walls; and (vii) exceeding shear capacity in walls. As an example, Fig 5 depicts the building response under R#5 at the onset of yield in slabs, yield in walls, and exceeding of wall rotation limit corresponded to Life Safety (LS) performance level, while Fig. 6 presents the response under R#3 at the onset of exceeding shear capacity in wall segments.

The main observations from the mapping process are:

- For both records, first yielding in steel rebars of RC flooring system occurred at the storey where maximum differential vertical displacement developed between slab ends. This is not necessarily the storey associated with maximum ISD.
- For R#5, the event sequence starts with yielding in the slab, followed by the following events in the wall: yielding, exceedance of LS rotation limit, rebar buckling, concrete crushing, exceedance of CP rotation limit, and finally exceedance of shear capacity. As above, the event sequence for R#3 starts with yielding in slab followed by yielding in wall. However, the sequence of the other events in the wall conspicuously differs with exceedance of shear capacity next, followed by rebar buckling, exceedance of LS rotation limit, concrete crushing, and ends with exceedance of CP rotation limit.
- For R#5, the shape of the relative lateral displacement plot at the onset of the sequence of events indicates a first mode-dominated response. However, the second mode appears responsible for the exceedance of the wall shear capacity event. On the contrary, for R#3, the shape of the relative lateral displacement plots indicate that the building response is controlled by the second mode except for wall yielding and shear capacity exceedance where the response is dominated by the third mode.
- By post-processing the analysis results, it is observed that the potential failure in wall segments when shear capacity is exceeded under the two records is differ in nature. Under both records, the maximum shear demand occurred at very low curvature ductility; 0.61/0.41 in 1st storey/2nd storey under R#5, and 0.06/0.06 in 1st storey/3rd storey under R#3. Notwithstanding this fact, the walls in the 1st and 2nd stories under R#5 have gone under a considerable amount curvature ductility (4.64 and 1.80, respectively) prior to the exceedance of shear capacity, while under R#3, the maximum curvature ductility in the walls at the 1st and 3rd stories were less than 1.0 (0.44 and 0.25, respectively). This indicates that under R#5, shear failure is preceded by flexural yielding in walls, giving the chance to flexure-related damages (strains and rotations) to occur first. While under R#3, wall segments in the concerned stories remain elastic (curvature ductility < 1) over the entire time history of the record at the seismic intensity level corresponded to the exceedance of shear capacity.
- For both seismic scenarios, at the onset of each of the damage events in the walls, seismic demands (strain/rotation/shear) reduce with building height, diminishing at the top five stories. This trend is inconsistent with the fact that these top stories are showing maximum overall Total Inter-Storey Drift (TISDs) during the damage sequence. This is examined further in the next section.

The above highlight the different nature of building response to the two seismic scenarios, vindicating the initial hypothesis of this paper.

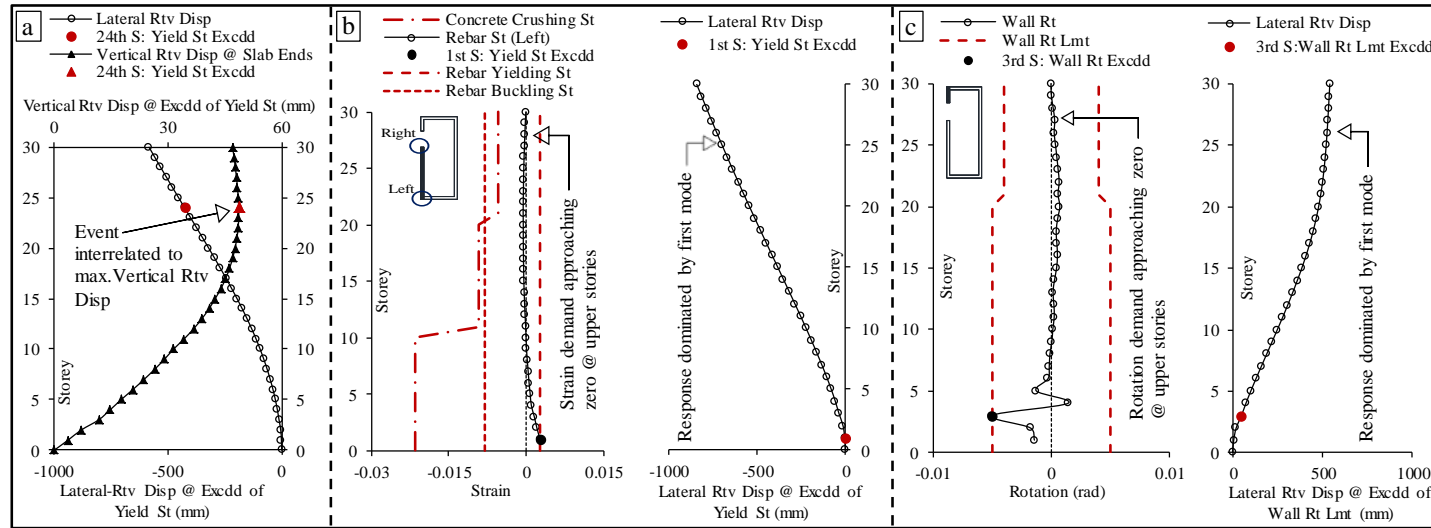


Fig. 5 – Sample building response to R#5: (a) rebar yielding in slabs; (b) rebar yielding in walls; and (c) ASCE/SEI 41-6 LS rotation limit in walls

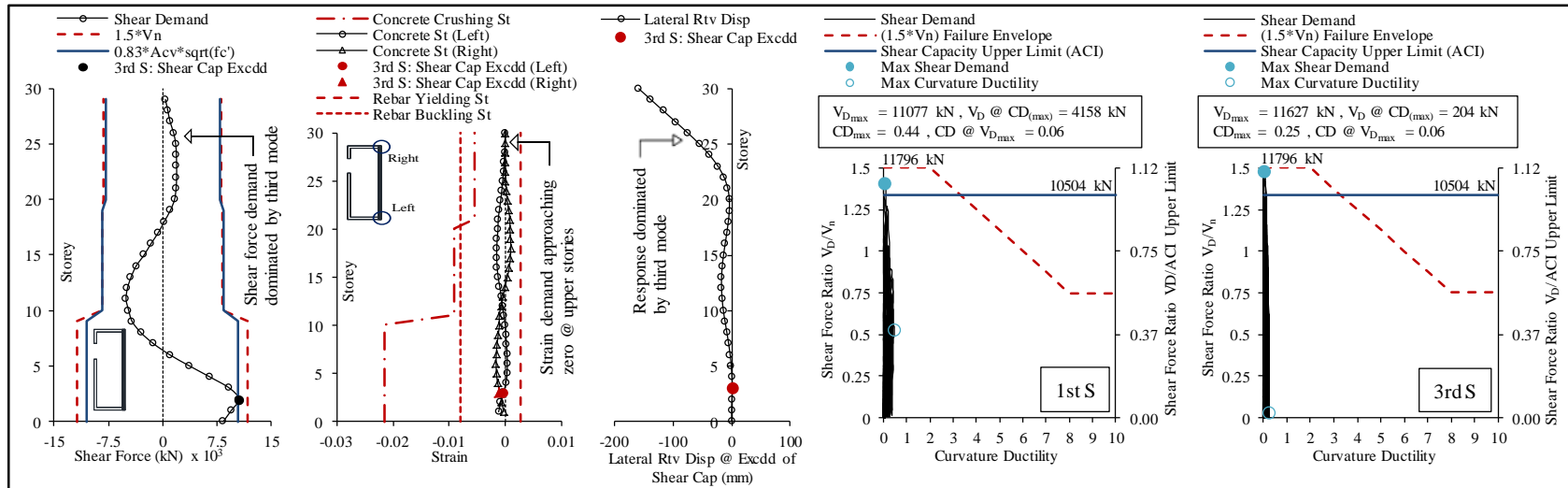


Fig. 6 – Sample building response to R#3: shear capacity exceedance in walls



7. Linking Local to Global Response

To quantitatively define performance limit states, DMs need to be adapted to link local-to-global response. The selection of DM depends primarily on the structural characteristics of the assessed building and its usage. DMs include: (i) deformation-based DMs such as roof drift and TISD; (ii) force-based DMs such as base shear; and (iii) energy-based DMs such as the global Park-Ang index [24]. TISD has been frequently used as a global DM in previous studies, since it is adopted by most of the seismic design and assessment provisions and can be easily calibrated against experimental data available in the literature.

TISD at any storey is a combination of two major components: (i) lateral net drift caused by shear and flexure deformation (NISD); and (ii) drift from Rigid Body Motion (RBM) caused by the rotation in lower storey (RBMISD). The former relates storey deformation to the stress and strain demands of members in that storey, while the latter has no contribution to structural demand. The contribution of RBM component to TISD is influenced by the location of the storey in the building, the total building height and the effect of higher modes on the seismic response. Ji et al. [25] illustrated that for high-rise buildings, the traditional DM of TISD is insufficient to be directly related to structural performance and therefore needs to be disaggregated to its main sources. This argument is further investigated in the present study. There are several methods available for calculating NISD including secant, improved secant, fixing floor and tangent [e.g. 26]. The latter method is adopted to calculate the NISD using post-processed element deformation data (mainly from the wall segment) as illustrated in Fig. 7 and Equation (1).

$$NISD_i = \frac{1}{h_i} \left\{ \frac{(THDisp_i - h_i \sin \theta_i)}{\cos \theta_i} + [NVDisp_i - h_i (1 - \cos \theta_i) - (THDisp_i - h_i \sin \theta_i) \tan \theta_i] \sin \theta_i \right\} \quad (1)$$

where $NISD_i$ is the NISD of the i^{th} storey, h_i is the height of the i^{th} storey, θ_i is tangent angle at the bottom end of the i^{th} storey, $THDisp_i$ is the total lateral (horizontal) displacement of the i^{th} storey, and $NVDisp_i$ is the net vertical displacement of the i^{th} storey. Fig. 8(a) shows TISD vs NISD envelopes for the sample building at selected seismic intensities. From both seismic scenarios and at all seismic intensities, it can be seen that NISD approaches zero at the top stories. This is consistent with the low seismic demands on the respective RC walls. The ratios of RBMISD to TISD at the onset of local damage events are plotted in Fig. 8(b). For R#5 and R#3, these ratios rise from 0.0 and 0.0 at the first storey, to an average of 0.91 and 0.70 at the twentieth storey, and 0.99 and 0.98 at the thirtieth storey, respectively. This confirms that at the higher storeys TISD is almost entirely dominated by RBMISD resulting from the rotation of lower storeys; hence there is practically no NISD and no damage.

To investigate the effect of building total height on the relationship between local damage events and drifts, a numerical parametric study is conducted. Maintaining the footprint and the geometry of the sample building, six more buildings with total number of stories of 20, 25, 35, 40, 45 and 50 (total height of 65.3m, 81.3m, 113.3, 129.3, 145.3, 161.3m, respectively) are designed and modelled as explained in Sections 2 and 4. Fig. 9 shows NISD and TISD at the onset of local damage events against building total height when subjected to R#5. Nearly all events, except exceedance of wall shear capacity occur at a similar NISD for all building heights. The NISD results for R#3 illustrate higher variability and this can be attributed again to the bigger impact of higher modes on the response of such buildings to near-field earthquakes.

TISD can be responsible for non-structural damage in tall buildings and inconvenience of the occupants, hence is important at least when evaluating the performance of high-rise buildings at serviceability level. However, the above discussion confirms that using NISD as a global DM for the vulnerability assessment of high-rise buildings is more appropriate due to its structural significance, its correlation with local response and its consistency in buildings with varying heights. Thus, it is decided to implement NISD as the global DM in this study.

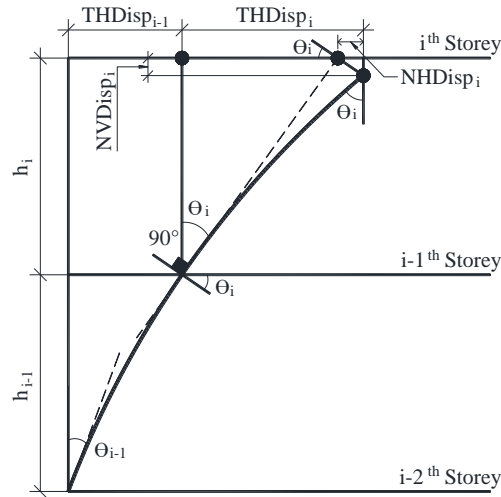


Fig. 7 – Member deformation shape for calculation of NISD

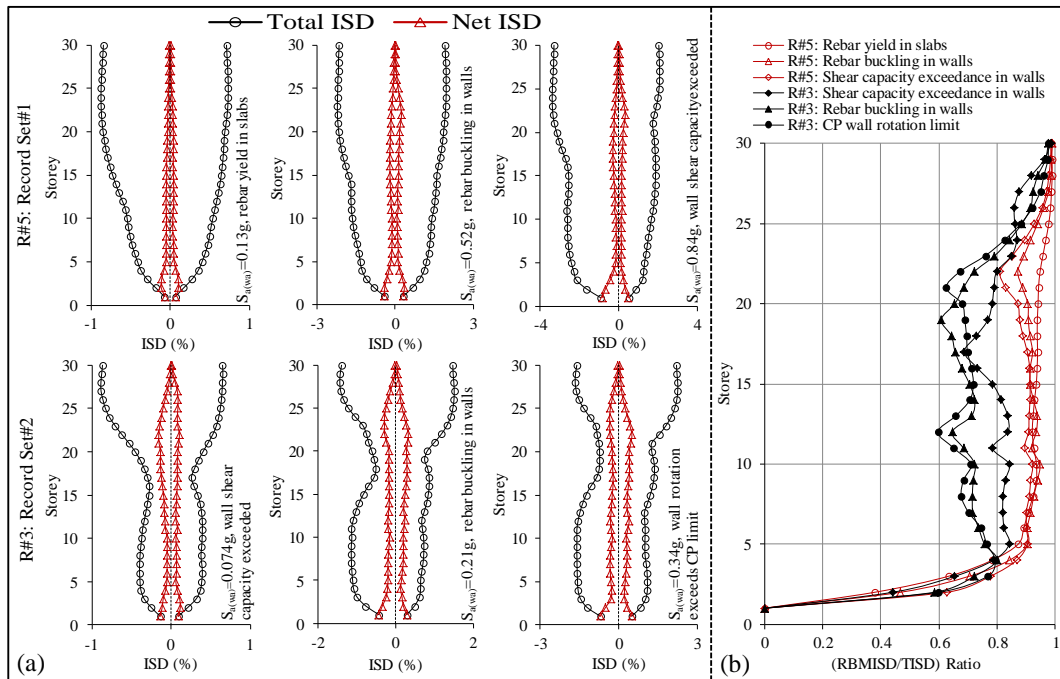


Fig. 8 – Sample building response: (a) TISD vs NISD envelopes; and (b) RBMISD to TISD ratio

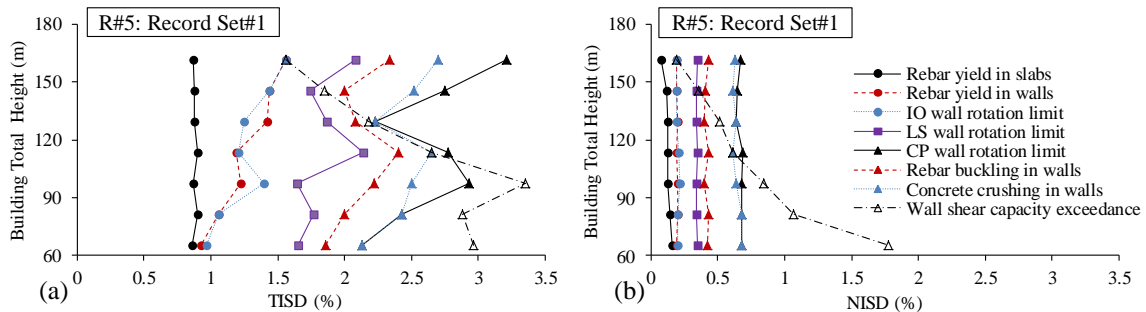


Fig. 9 – R#5: Response of buildings with different height at the onset of DIs: (a) TISD; and (b) NISD



8. Definition of Performance Limit State Criteria

The three commonly used performance levels, Immediate Occupancy (IO), LS and Collapse Prevention (CP), are adopted in the present study, but new SSSB limit state criteria are proposed using the MRIDAs results from the 40 selected records and the mapping/linking of predefined local damages discussed in Sections 6 and 7. Fig. 10 depicts the 50% fractile of the NISDs related to selected local damage events (or combination of events) under R#5 and R#3. The proposed limit state criteria associated with the two studied seismic scenarios are discussed in the succeeding sub-sections.

8.1 Limit states for severe distant earthquake scenario

For this scenario, the 50% fractile of the NISDs associated with the first reinforcing steel yield in the flooring system is 0.11% (Fig. 10(a)). This value is selected as the IO limit state in the present study. Although the 50% fractile TISD (0.81%) corresponding to this value is higher than that suggested by ASCE/SEI 41-06 (0.5%), it is justified by the fact that the structural system of the sample building (piers and core walls with flat slabs) has potentially larger deformations when compared with structures employing other flooring systems. For first yield in walls the 50% fractile of the NISDs is 0.19% (corresponding to 50% fractile TISD=1.43%). Again this relatively high NISD value is attributed to the high compressive load on the lower stories, which delays the onset of initial yielding and cracking of vertical elements.

For the CP limit state, the 50% fractile of the NISDs associated with all monitored CP-related damage events with and without considering shear demand/supply local damage index are 0.37% and 0.44% (corresponding to 50% fractile TISD=2.39% and 2.72%), respectively. In 11 out of the 20 input ground motions, shear wall capacity, particularly of core segments at lower stories, is exceeded prior to the onset of any other CP-related damage events. This is attributed to the increasing influence of higher modes on the structural response at higher input ground motion intensities. Hence, the NISD associated with the CP limit state is taken as 0.37%.

The adopted criteria for reaching the LS limit state are either the wall rotation limit according to ASCE/SEI 41-6 or 50% of the NISD associated with all CP-related deformation-based DIs, whichever comes first. As shown in Fig. 10(a), the 50% fractile of NISD associated with wall rotation is 0.30% (corresponding to 50% fractile TISD=2.09%), while the 50% NISD of the deformation-based DIs corresponding to CP is calculated as 0.22%. Hence, the latter value is selected as the level of NISD that is corresponding to the LS limit state.

8.2 Limit states for moderate near-field earthquake scenario

For this scenario, the response of the sample building differs significantly from before since the high frequencies and short durations of the input ground motions render higher modes dominate the building response. Building response under R#5 is dominated by the first mode (except in shear capacity exceedance) while under R#3, response to all events is dictated by the second or third mode. In fact, higher modes shift the shear wall response from flexure-controlled under Record Set#1 to shear-controlled under Record Set#2. This is confirmed by the NISD distribution shown in Fig. 10(b), where shear capacity is exceeded in core segments at lower stories prior to the detection of the first plastic hinge anywhere in the structure in 8 out of 20 records and before the first plastic hinge is initiated in wall elements in 15 out of 20 records. As shown in Fig. 10(b), the calculated 50% fractile NISD associated with the shear capacity damage index is 0.15%. This value corresponds to 50% fractile TISD=0.79%; a value close to the TISD suggested by ASCE/SEI 41-6 for walls with shear-controlled response at CP (0.75%).

Based on the above, NISD values of 0.08% and 0.11% are proposed to be associated with IO and LS limit states, respectively. These values correspond to the TISDs (0.4% and 0.6%) recommended in ASCE/SEI 41-6 for walls with response controlled by shear. For CP, NISD of 0.15% is proposed. The mapped and proposed limit state criteria for the building under Record Set#1 and Record Set#2 are listed in Table 1.

Table 1– Mapped and proposed limit state criteria for the sample building

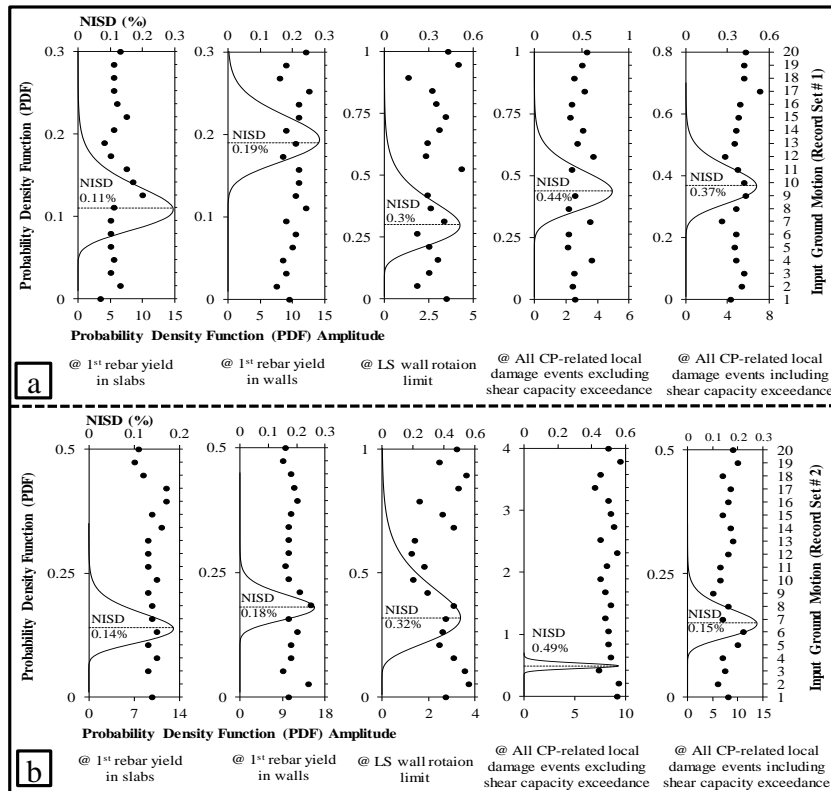


Fig. 10 – 50% fractile of NISDs associated with selected local damage events obtained from MRIDAs of the sample building: (a) Record Set#1; and (b) Record Set#2

Limit state	Damage Index (DI)	NISD (%)			
		Record Set#1		Record Set#2	
		Mapped	Proposed	Mapped	Proposed
IO	rebar yield in slabs	0.11		0.14	
	rebar yield in walls	0.19		0.18	
	Wall rotation limit (ASCE/SEI 41-6)	0.19		0.17	
	All IO-related deformation-based DIs (combined)	0.11	0.11	0.14	0.08
	NISD corresponding to value in Table 6-19 of ASCE/SEI 41-6 for RC shear walls controlled by shear	N/A		0.08	
	Wall rotation (ASCE/SEI 41-6)	0.30		0.32	
LS	50% of NISD from all CP-related deformation-based DIs (combined)	0.22	0.22	0.25	0.11
	NISD corresponding to value in Table 6-19 of ASCE/SEI 41-6 for RC shear walls controlled by shear	N/A		0.11	
		1st rebar buckling in walls	0.44		0.49
CP	1st concrete crushing in walls	0.59		0.67	
	Wall rotation (ASCE/SEI 41-6)	0.51		0.71	
	Shear capacity exceedance	0.34		0.15	
	All CP-related deformation-based DIs (combined)	0.44	0.37	0.49	0.15
	All CP-related DIs inclusive of shear capacity (combined)	0.37		0.15	
	NISD corresponding to value in Table 6-19 of ASCE/SEI 41-6 for RC shear walls controlled by shear	N/A		0.14	

9. Fragility Relations and Performance Limit States Exceedance Probability

To illustrate the use of the proposed SSSB limit state criteria, two sets of fragility relations are developed (Fig. 11(a)). The developed fragility relations depict the probability of the sample building to exceed different PLSs under the two investigated seismic scenarios. The PLSs exceedance probabilities at the spectral acceleration corresponding to the design and twice the design levels are illustrated in Fig. 11(b). Under the severe distant earthquake scenario (Record Set#1), Fig. 11(b) shows that at spectral acceleration corresponding to the design level, the probability of exceeding the IO, LS and CP PLSs is 38.0%, 7.0% and 1.0%, respectively. At spectral acceleration corresponding to twice the design level, these values increase to 78%, 37% and 11%, respectively. The presented sample results illustrate the significance of the proposed SSSB limit state criteria for developing reliable fragility relations and emphasize the higher vulnerability of RC high-rise wall buildings to far-field earthquakes.

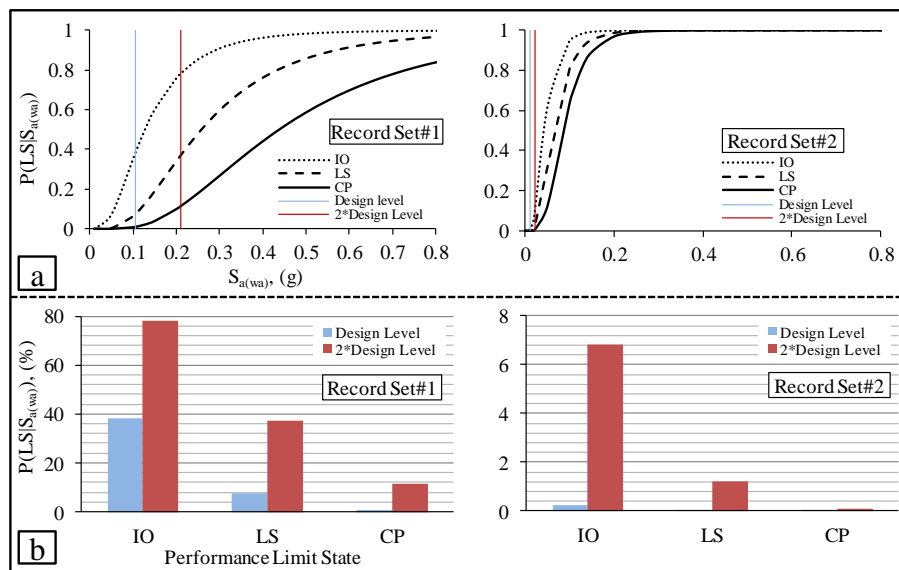


Fig. 11 – Fragility relations and PLS exceedance probability for the sample building: (a) fragility relations; and (b) PLS exceedance probability

10. Summary and Conclusions

This study develops a methodology for reliable Seismic Scenario-Structure-Based (SSSB) definitions of performance limit state criteria for high-rise RC wall buildings. The methodology is illustrated on a 30-storey RC wall sample building located in Dubai (study region). Multi-Record Incremental Dynamic Analyses (MRIDAs) with new intensity measure are conducted to assess building local response to two different seismic scenarios. Seismic scenario-based local damages, presented with a range of deformation and capacity-based damage indices, are mapped and linked to building global response. Finally, a new set of SSSB limit state criteria is proposed for the sample structure. A parametric study involving the sample 30-storey building in addition to six other buildings with different heights shows that, for such buildings, NISD is a more reliable global damage measure compared with TISD for use in defining limit state criteria. NISD is better linked with the local response over the height of the building and well correlated to deformation-based local damage events for buildings with varying heights. The study shows that structural system, arrangement and geometry of vertical elements and axial force level in the lower stories influence the seismic intensity and deformation levels that are related to local damage events. It is found that near-field earthquake events can shift the seismic response from flexure-controlled to shear-controlled. This leads to the conclusion that the response of RC high-rise wall buildings and consequently the definition of limit state criteria for designated performance levels are strongly influenced by both the structure and the seismic scenario. As a result, new SSSB limit state criteria are proposed for RC high-rise wall buildings in seismic regions.



11. Acknowledgments

This work was partially supported by the United Arab Emirates University under research grant 31N227.

12. References

- [1] Abdalla JA, Al-Homoud AS (2004): Seismic hazard assessment of United Arab Emirates and its surroundings. *Journal of Earthquake Engineering*, **8** (06), 817-837.
- [2] Sigbjörnsson R, Elnashai AS (2006): Hazard assessment of Dubai, United Arab Emirates, for close and distant earthquakes. *Journal of Earthquake Engineering*, **10** (05), 749-773.
- [3] DMA-AD (2013): *Abu Dhabi International Building Code*. Department of Municipal Affairs, Abu Dhabi, UAE.
- [4] ACI (2014): *Building code requirements for structural concrete (ACI 318M-14) and commentary*. American Concrete Institute, Farmington Hills, MI.
- [5] Mwafy A, Elnashai AS, Sigbjörnsson R, Salama A (2006): Significance of severe distant and moderate close earthquakes on design and behavior of tall buildings. *The Structural Design of Tall and Special Buildings*, **15** (4), 391-416.
- [6] Ambraseys N, Douglas J, Sigbjörnsson R, Berge-Thierry C, Suhadolc P, Costa G, Smit M (2004): Dissemination of European strong-motion data, Volume 2, using strong-motion dataspaces navigator, CD ROM collection. *Proceedings of the The Proceedings of the 13th World Conference on Earthquake Engineering*, Vancouver, Canada.
- [7] PEER (2014): *Ground motion database*. Pacific Earthquake Engineering Research Center, <http://peer.berkeley.edu/nga>.
- [8] CSI (2011): *PERFORM-3D V5: Nonlinear analysis and performance assessment for 3D structures: User Manual*. Computer and Structures, Inc., 1995 University Avenue, Berkeley, CA.
- [9] Alwaeli W, Mwafy A, Pilakoutas K, Guadagnini M (2014): Framework for developing fragility relations of high-rise rc wall buildings based on verified modelling approach. *Proceedings of the Second European Conference on Earthquake Engineering and Seismology*, Istanbul, Turkey.
- [10] Panagiotou M, Restrepo JI, Conte JP (2007): *Shake table test of a 7 story full scale reinforced concrete structural wall building slice phase I: Rectangular Wall Section*. Department of Structural Engineering, University of California San Diego, CA.
- [11] Panagiotou M, Restrepo JI, Conte JP (2011): Shake-table test of a full-scale 7-story building slice. Phase I: Rectangular wall. *Journal of Structural Engineering*, **137** (6), 691-704.
- [12] LATBSDC (2011): *An alternative procedure for seismic analysis and design of tall buildings located in the los angeles region*. Los Angeles Tall Buildings Structural Design Council, Los Angeles, CA.
- [13] Martínez-Rueda JE, Elnashai AS (1997): Confined concrete model under cyclic load. *Materials and Structures*, **30** (3), 139-147.
- [14] Orakcal K, Wallace JW (2006): Flexural modeling of reinforced concrete walls-experimental verification. *ACI Structural Journal*, **103** (2), 196-206.
- [15] Tuna Z (2012): Seismic Performance, Modeling, and Failure Assessment of RC Shear Wall Buildings. *PhD Thesis*, University of California.
- [16] Bae S, Miseses AM, Bayrak O (2005): Inelastic buckling of reinforcing bars. *Journal of structural engineering*, **131** (2), 314-321.
- [17] Cosenza E, Prota A (2006): Experimental behaviour and numerical modelling of smooth steel bars under compression. *Journal of Earthquake Engineering*, **10** (3), 313-329.
- [18] Rodriguez ME, Botero JC, Villa J (1999): Cyclic stress-strain behavior of reinforcing steel including effect of buckling. *Journal of Structural Engineering*, **125** (6), 605-612.
- [19] ASCE (2007): *ASCE/SEI 41-06: Seismic rehabilitation of existing buildings*. American Society of Civil Engineers, Reston, VA.
- [20] Thomsen JH, Wallace JW (2004): Displacement-based design of slender reinforced concrete structural walls-experimental verification. *Journal of Structural Engineering*, **130** (4), 618-630.
- [21] Gogus A (2010): Structural wall systems-nonlinear modeling and collapse assessment of shear walls and slab-column frames. *PhD Thesis*, University of California.
- [22] Orakcal K, Massone LM, Wallace JW (2009): Shear strength of lightly reinforced wall piers and spandrels. *ACI Structural Journal*, **106** (4), 455-465.
- [23] Satake N, Suda K, Arakawa T, Sasaki A, Tamura Y (2003): Damping evaluation using full-scale data of buildings in Japan. *Journal of structural engineering*, **129** (4), 470-477.
- [24] Park Y-J, Ang H-S (1985): Mechanistic seismic damage model for reinforced concrete. *Journal of Structural Engineering*, **111** (4), 722-739.
- [25] Ji J, Elnashai AS, Kuchma DA (2009): Seismic fragility relationships of reinforced concrete high-rise buildings. *The Structural Design of Tall and Special Buildings*, **18** (3), 259-277.
- [26] Cai J, Bu G, Yang C, Chen Q, Zuo Z (2014): Calculation Methods for Inter-Story Drifts of Building Structures. *Advances in Structural Engineering*, **17** (5), 735-746.